



Journal of Rehabilitation in Civil Engineering

Journal homepage: <https://civiljournal.semnan.ac.ir/>

Improving Stability and Buckling Resistance of Self-Supporting Isotrussed Telecommunication Tower under Wind Load: An Evaluation According to TIA-222-G Standards

Mahamoudou Faharidine ^{1,2,*}; Muhammad Usama Aslam ^{1,3}; Mohamed Moutuou Choufaikat ⁴

1. Department of Disaster Mitigation for Structures, College of Civil Engineering, Tongji University, Shanghai 200092, China
 2. Department of Construction Management and Real Estate, School of Economics and Management, Tongji University, Shanghai 200092, China
 3. Department of Civil Construction and Environmental Engineering Ames, Iowa State University, Iowa 50011, Unites States
 4. Department of Mathematics, Faculty of Sciences and Letters, Aksaray University, Aksaray 68100, Turkey
- * Corresponding author: fahar@tongji.edu.cn

ARTICLE INFO

Article history:

Received: 06 March 2024

Revised: 23 June 2024

Accepted: 02 November 2024

Keywords:

Isotruss;

Telecommunication tower;

Wind loads;

Stability;

TIA-222-G.

ABSTRACT

Despite the growing demand for durable telecommunication infrastructure, tower stability and durability remain significant challenges. The self-supporting isotrussed telecommunication tower (SSITT) offers a promising solution, but its performance under wind loads requires further improvements. This paper investigates SSITT stability and provides guidelines for wind load calculations based on the Telecommunications Industry Association Standard 222 Revision G (TIA-222-G). The isotruss, a lightweight lattice structure made from advanced composite materials, is analyzed using ABAQUS finite element software. Two 10 m 8-node SSITTs, using carbon/epoxy as the material, were modeled. The results show that the maximum displacements of 45.17 mm (Model 1) and 47.29 mm (Model 2) at the top are within acceptable limits, while the maximum stresses of 135.6 MPa (Model 1) and 198.9 MPa (Model 2) are below the material's limit of 306 MPa. The study found that the longitudinal member experiences the highest stress levels, which may lead to buckling. To improve performance and durability, it is recommended that the longitudinal member be designed with a larger radius than the helical member.

E-ISSN: 2345-4423

© 2025 The Authors. Journal of Rehabilitation in Civil Engineering published by Semnan University Press.

This is an open access article under the CC-BY 4.0 license. (<https://creativecommons.org/licenses/by/4.0/>)

How to cite this article: Faharidine, M. , Aslam, M. Usama and Choufaikat, M. M. (2025). Improving Stability and Buckling Resistance of Self-Supporting Isotrussed Telecommunication Tower under Wind Load: An Evaluation According to TIA-222-G Standards. Journal of Rehabilitation in Civil Engineering, 13(3), 54-13. <https://doi.org/10.22075/jrce.2024.33439.2013>

1. Introduction

In recent years, the use of fiber-reinforced polymer (FRP) composites as an alternative to traditional materials in infrastructure has gained significant attention [1]. This interest is driven by the many advantages offered by FRP materials over their traditional counterparts. For instance, FRP composites exhibit exceptional environmental resilience, high stiffness and strength-to-weight ratios, and great fatigue and corrosion resistance [2,3]. These material properties translate into a host of cost-performance advantages when used for structural applications [4-6], but they also allow for quick installation times, lower maintenance costs, and longer lifetimes compared to traditional materials [7]. FRP composites are composed of a polymer matrix and engineered fibers, creating a synergy that leverages the best qualities of both components [8, 9]. The matrix, often made from thermosetting resins like epoxy, polyester, or vinyl ester, binds and protects the fibers—typically glass, carbon, or aramid—distributing loads and imparting durability [9, 10]. The fibers provide the composite with remarkable strength and stiffness, crucial for the structural integrity of infrastructure projects. Moreover, FRP composites can be engineered to achieve specific performance criteria by varying the composition and arrangement of constituent materials [12]. This customization capability is pivotal, allowing designers and manufacturers to tailor FRP composites to meet the unique needs of each project. The ability to vary fiber type, orientation, and volume fraction, along with the choice of matrix material, offers a versatile solution to a wide range of engineering challenges, ensuring that FRP composites remain at the forefront of materials technology in infrastructure development [13].

The telecommunications industry is one sector that has seen the benefits of using FRP composites for infrastructure development [14]. Telecommunication towers are essential components of the communication network, and they are required to withstand environmental loads such as wind, snow, and ice. Conventionally, telecommunication towers have been made of steel, but in recent years, FRP composites have emerged as a viable alternative [13]. However, the use of FRP materials in telecommunication tower design requires careful consideration and analysis to ensure their safe and reliable performance. Due to the unique properties of FRP composites, design standards and guidelines such as TIA-G-222 (guidelines for antenna supporting structures) [16], EN 1993-3-1 (European standard for steel tower design) [17], GB 50135-2006 (Chinese standard for high-rise structures) [18], and CSA S37-18 (Canadian standard for antenna-supporting structures) [19] are necessary to analyze towers made from these materials. These standards provide guidelines for the design, construction, and testing of telecommunication towers to ensure their structural integrity and stability under various loading conditions, including wind, seismic, and environmental loads. In addition, these standards specify the materials, fabrication, and installation requirements to ensure the towers' long-term durability and reliability.

An isotruss is a three-dimensional truss structure composed of interconnected triangular units [20], developed by Dr. David W. Jensen, a professor at Brigham Young University in collaboration with NASA in 1994. This design optimizes the use of composite materials in lightweight structures without compromising strength [21]. Its primary components include nodes—joint connections—and straight members that form the triangle edges, each configured into sections called 'bays' that are customizable for specific mechanical properties and applications [22]. Materials typically used for manufacturing Isotruss structures include high-performance composites like carbon fiber-reinforced polymer (CFRP) or glass fiber-reinforced polymer (GFRP). These materials are chosen for their high strength-to-weight ratios and excellent corrosion resistance, which are critical for applications in demanding environments such as aerospace, construction, and telecommunications

[23]. Since its inception, ongoing research has been conducted to advance the manufacturing techniques [24], predict failure modes using analytical [24, 25] and numerical methods [27-29], and explore specific applications [30-32]. The Isotruss geometry has been employed in various industries and for multiple uses, including reinforced concrete beams [33], piles [27], columns [33], bridges [34], and bicycle frames [35]. The unique arrangement of fibers aligned with the direction of force enhances the material's isotropic properties, making it transversely isotropic [36]. This fiber alignment not only maximizes the material's strength in the direction of stress but also maintains uniform properties across different directions, which is crucial for maintaining integrity under varied load conditions. This geometric and material configuration offers significant advantages including resistance to shell buckling—a prevalent issue in thin-walled structures—owing to the repeating pattern of triangles [37]. Moreover, the isotruss structure exhibits lower drag forces compared to traditional solid-wall designs, providing benefits in both aerodynamic and hydrodynamic scenarios [38], as illustrated in Fig. 1. The triangular pattern also contributes to increased damage tolerance and redundancy, further enhancing the structural reliability of Isotruss applications [40, 41].

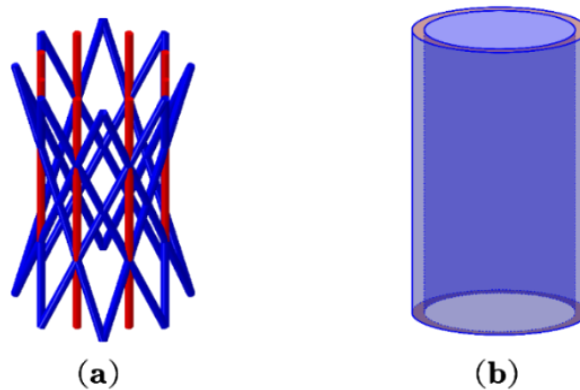


Fig. 1. Shell buckling resistance and drag force interpretation: (a) isotruss geometry, (b) solid-walled cylindrical tube.

Isotruss technology is particularly suited to the telecommunications industry because of its lightweight and unique design, resulting in lower installation, maintenance, and transportation costs [41]. Isotruss is ideal for locations with harsh weather conditions, such as coastal regions with high humidity, hurricane-prone regions, and locations with difficult access for maintenance and repair, because it does not rust or rot. Compared to steel towers, which may need to be replaced after only 5 years, Isotruss towers can last 50 years or more in such areas [42].

The present study investigates the stability of two different SSITT configurations that differ only in the bay length, with the second configuration having nearly half the length of the first (0.625 m and 0.3125 m). The configuration of the isotruss structure has a direct impact on its total mass, which is an important consideration for tower design. The primary goal of this study is to evaluate the stability of the SSITT under wind loads following TIA-222-G and to provide guidelines for calculating wind loads. This work has been previously conducted for different tower structures by Rasool et al. [43]. The tower structure is modeled using ABAQUS [44] to study under two conditions: the ultimate limit state and the serviceability limit state. The results of this study will contribute to the development of SSITTs for telecommunications and other industries where lightweight and durable structures are required.

2. Data analysis

To evaluate the stability of the SSITT, two computer models of the towers were developed and subjected to both dead loads and wind loads. The wind loads were calculated following the TIA-222-G standard, while the dead load on the towers was kept constant. The tower configuration that was specified for the SSITT was used to create these models, along with analysis software deemed most suitable for the task. The software simulated the behavior of the towers under different loading conditions, enabling an assessment of their stability and performance. Additionally, careful consideration was given to the deadload applied to the towers during the analysis to ensure that the results accurately reflected the tower's behavior under normal operating conditions.

2.1. Tower configuration

This study presents an analysis of 10-meter self-supporting isotrussed towers. As shown in Fig. 2(a), isotruss is a one-dimensional (1D) grid structure composed of longitudinal members that are distributed longitudinally along the structure, and the helical members spiral along the broken line of the axial direction of the structure to form a periodic rolling profile. Fig. 2(a) illustrates the construction of the structure, which consists of numerous sections or bays. From the top view of the eight-node Isotruss structure in Fig. 2 (b), the top view of the tower presents two misplaced squares, with the nodes corresponding to the vertices of the squares and the longitudinal grid bars passing through the intersection of the two squares. The general configuration of the tower is shown in Fig.2, while the specific member sizes are detailed in Table 1.

Table 1. General arrangement and member size.

Model	Tower length $H(m)$	Outer radius $R(m)$	Member radius $r(m)$	Bay length $L_B(m)$	Number of sections n_{sec}	Angle $\phi(^{\circ})$
Model 1	10	0.18	0.009	0.625	16	67.839
Model 2	10	0.18	0.009	0.3125	32	50.834

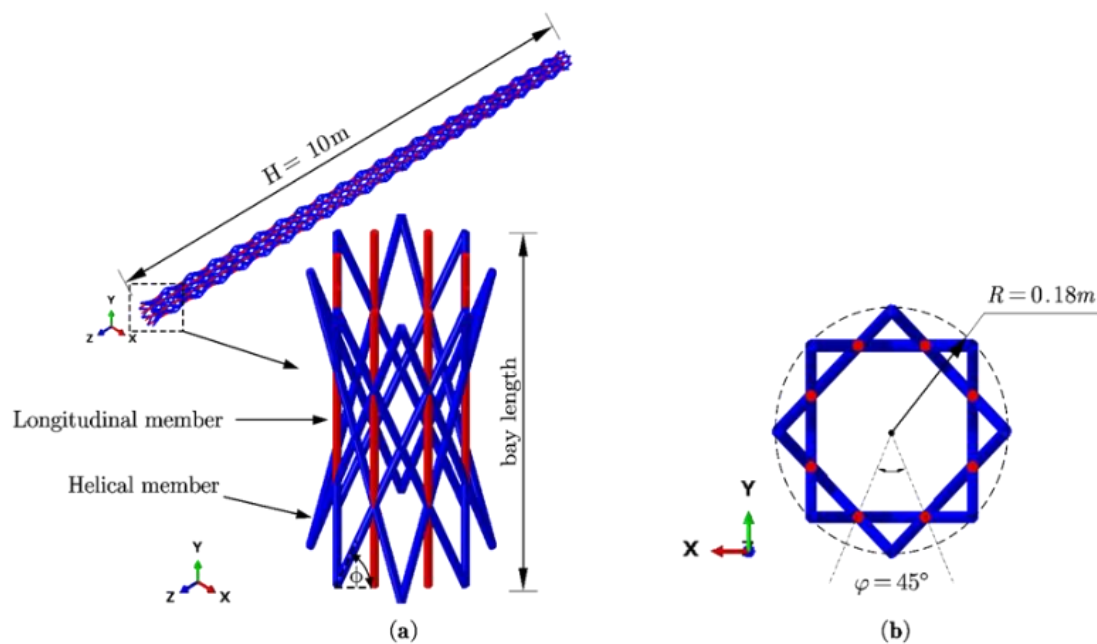


Fig. 2. Tower configuration: (a) tower section (bay), (b) top view.

2.2. Analysis software

To simulate the tower model numerically, a finite element analysis (FEA) was performed using the FE application ABAQUS. The modeling of the longitudinal and helical members of the Isotruss was achieved using the quadratic three-node beam element B32. This element is well-suited for the geometrically nonlinear analysis of truss structures and can be applied to evaluate thin to moderately thick beams. The tower was modeled with free-fixed boundary conditions. Two load combinations have been considered for analysis according to the limit state condition:

Ultimate limit state (ULS) condition:

$$1.2D + 1.6W_0 \quad (1)$$

Where D is dead load of the structure and W_0 the wind load.

Serviceability limit state (SLS) condition:

$$1.0D + 1.0W_0 \quad (2)$$

Where D is dead load of the tower and W_0 the wind load.

The towers are segmented into eight sections, and Table 2 displays the first section (0-1.25m) details.

Table 2. Tower weight and area.

Model	Level (m)	Ht.(m)	Height from ground to centerline Z(m)	Tower mass (Kg)	Gross area of tower face of mounting frame $A_g(m^2)$	Flat structural components projected area $A_f(m^2)$
Model 1	0-1.25	1.25	0.625	10.9375	0.45	0.23575
Model 2	0-1.25	1.25	0.625	15.25	0.45	0.264125

2.3. Dead loads on the tower

The tower's deadloads consist of two components: the self-weight of the tower and the weight of the equipment to be installed on it. The self-weight of the tower can be calculated from the values provided in Table 2, which considers the size and geometry of the tower components. To accurately calculate the tower's self-weight, the material constants of the carbon/epoxy material, obtained from Rackliffe [41] and presented in Table 3, were used. These constants provide essential information about the mechanical properties of the material, which are required for calculating the self-weight of the tower. Using Eq. (3) so the self-weight of tower 1 and 2 are 858.375 KN and 1196.82 KN, respectively.

In addition to the self-weight of the tower, the weight and dimensions of the equipment to be installed must be considered. Specifically, a TDD 8T8R antenna (dimensions: 1050 mm × 288 mm × 118 mm, 10.5 kg) is installed at 8.5 meters.

The overall self-weight of the tower model 1 and model 2 are 868.875KN and 1217.32 KN, respectively.

Table 3. Carbon/Epoxy material nominal properties.

Property [Unit]	Symbol	Value
Density [$lb./in.^3$ (Kg/m^3)]	ρ	0.049(1360)
Elastic modulus [ksi (GPa)]	E_1, E_2, E_3	23300(161), 966(6.66),
Poisson ratio	$\nu_{zr}, \nu_{z\theta}, \nu_{\theta r}$	0.32, 0.32, 0.33
Shear modulus [ksi (GPa)]	$G_{z\theta}, G_{zr}, G_{\theta r}$	432(2.98), 432(2.98), 364(2.51)

3. Wind load calculations and analysis

The impact of wind loads on towers and antennas can result in abnormal structural deformation. The TIA-222-G standard provides guidelines for accounting for load amplification due to wind gusts that resonate with the self-supporting structure's along-wind vibrations. ABAQUS was utilized to evaluate the tower structure based on the wind load calculations.

3.1. Tower configuration and general parameter

The wind load in TIA-222-G is based on 3 – secgust (a 50 – yr return). Due to space limitations, the wind forces are computed here for a basic wind speed of 150kph Structure Class-I as per relations given in TIA-222-G. The factors include basic wind speed $V = 150Kph = 41.7 m/s$, importance factor, $I = 0.87$ (Structure Class-I), exposure category= C , velocity pressure coefficient, K_Z (see Eq.(3)), $K_{Zmin} = 0.95$, topographic factor, $K_{Zt} = 1.0$ (Topographic Catagory-1), wind direction probability factor, $K_d = 0.85$, gust effect factor, $G_h = 0.85$ for $h = 10m < 137m$, velocity pressure (see Eq.(4)).

$$K_Z = 2.01(Z/Z_g)^{2/\alpha} \quad (3)$$

$$(q_z) = 0.613K_ZK_{Zt}K_dV^2I(N/m^2) \quad (4)$$

Two models have been developed as shown in Table 1 and the solidity ratio (ϵ) is calculated using the relation:

$$\epsilon = (A_f + A_r)/A_g \quad (5)$$

Where A_f is the projected area of flat structural components, A_g is the gross area of one tower face is calculated as shown and A_r is the projected area of round structural components $A_r = 0$, as there are no round members.

3.2. Effective projected area (EPA)

The effective projected area $(EPA)_S$ of tower segments is calculated in Table 4, with reference to Fig. 3. Using Eq. (7), the wind force is assumed to be applied at an angle of 0° . The formula for $(EPA)_S$ is given by:

$$(EPA)_S = C_f[D_f\sum(D_fA_f) + D_r\sum(A_rR_r)] \quad (6)$$

Where C_f is the force coefficient for a structure, D_f is wind direction factor for flat structural components, D_r is the wind direction factor for round structural components, and R_r is reduction factor for a round element in a tower face $C_f = 4.0\epsilon^2 - 5.9 + 4.0$.

The projected area of one bay (see Fig. 3) is as follows:

$$A = n_{sec}A_B \tag{7}$$

Where A is Full tower projected area, A_B is projected area of a bay and n_{sec} denotes numbers of sections (bays).

The effective projected area of the antenna $(EPA)_A$ is calculated as the formula below:

$$(EPA)_A = C_a A_a \tag{8}$$

where C_a is force coefficient for the appurtenance and A_a is the projected area of the appurtenance.

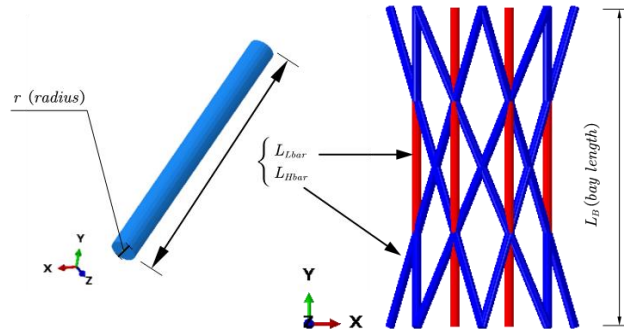


Fig. 3. projected area calculation.

Table 4. Effective projected area $(EPA)_S$.

Model	solidity ratio ϵ	force coefficient C_f	projected area $A_f(m^2)$	wind direction factor $D_f(0^\circ)$	$(EPA)_S(0^\circ)(m^2)$
Model 1	0.5239	2.0069	0.2358	1.0000	0.4731
Model 2	0.5869	1.9150	0.2641	1.0000	0.5058

Table 4 shows the values of one section of the two models.

3.3. Wind force on the tower.

The wind force on the structure F_{ST} and the appurtenance F_A are calculated using the following equations, respectively:

$$F_{ST} = (q_z)_S G_h (EPA)_S \tag{9}$$

$$F_A = (q_z)_A G_h (EPA)_A \tag{10}$$

From Eq. (4) the velocity pressure coefficient K_Z varies according to the height Z . Using exposure category C , means the coefficients $\alpha = 9.5$ and $Z_g = 274m$.

3.3.1. Ultimate limit state condition (ULS)

As per the standard requirements, structures must be designed to ensure their design strength surpasses or is equivalent to the load effects of the factored loads for every limit state combination. Table 5 provides information on the wind load experienced by the tower under ultimate limit state (ULS) conditions, employing the combination specified in Eq.(1)

A TDD 8T8R antenna (1050×288×118) is attached at 8.5 m to the tower body. Using both Eqs. (9) and (11), deriving C_a from TIA-222-G in Table 2-8: $F_A = 0.2728kN(0^\circ)$.

The total design wind load, F_W , should be determined according to the following:

$$F_W = F_{ST} + F_A \tag{11}$$

Table 5. Design wind force on the tower body as per TIA-222-G.

Section	Level (m)	Velocity pressure coefficient (K_z)	Velocity pressure $q_z(kN/m^2)$	Model 1	Model 2
				$F_{ST}(0^\circ)(kN)$	$F_{ST}(0^\circ)(kN)$
8	8.75-10	0.9838	0.8667	0.3486	0.3726
7	7.5-8.75	0.9545	0.8409	0.3382	0.3616
6	6.25-7.5	0.9215	0.8118	0.3265	0.3490
5	5-6.25	0.8833	0.7782	0.3129	0.3346
4	3.75-5	0.8376	0.7380	0.2968	0.3173
3	2.5-3.75	0.7802	0.6874	0.2764	0.2955
2	1.25-2.5	0.7005	0.6172	0.2482	0.2653
1	0-1.25	0.5556	0.4895	0.1968	0.2104

3.3.2. Serviceability limit state (SLS) condition

According to the TIA-222-G, the horizontal wind forces for determining service loads shall be based on an importance factor, I , of 1.00, for a 60mph [27m/s] basic wind speed, and a directionality factor, K_d , of 0.85 for all structures. The velocity pressure coefficient, K_z , the gust effect factor, G_h , and the topographic factor, K_{zt} , shall be equal to the values for the ultimate limit state condition. Table 6 presents the wind force in the SLS condition.

The wind loads in the ABAQUS model were applied using the concentrated load approach. This method involves dividing the pole into multiple sections and applying the calculated wind load for each section as a concentrated force at the midpoint of the section. This approach ensures an accurate representation of the wind forces acting on the pole while simplifying the modeling process. Fig. 5 illustrates the application of these concentrated wind loads at various heights along the pole.

Table 6. Service limit state wind force as per TIA-222-G.

Section	Level (m)	Velocity pressure coefficient (K_z)	Velocity pressure $q_z(kN/m^2)$	Model 1	Model 2
				$F_{ST}(0^\circ)(kN)$	$F_{ST}(0^\circ)(kN)$
8	8.75-10	0.9946	0.3737	0.1503	0.1607
7	7.5-8.75	0.9670	0.3626	0.1458	0.1559
6	6.25-7.5	0.9361	0.3500	0.1408	0.1505
5	5-6.25	0.9007	0.3355	0.1349	0.1442
4	3.75-5	0.8593	0.3182	0.1280	0.1368
3	2.5-3.75	0.8087	0.2964	0.1192	0.1274
2	1.25-2.5	0.7424	0.2661	0.1070	0.1144
1	0-1.25	0.6414	0.2110	0.0849	0.0907

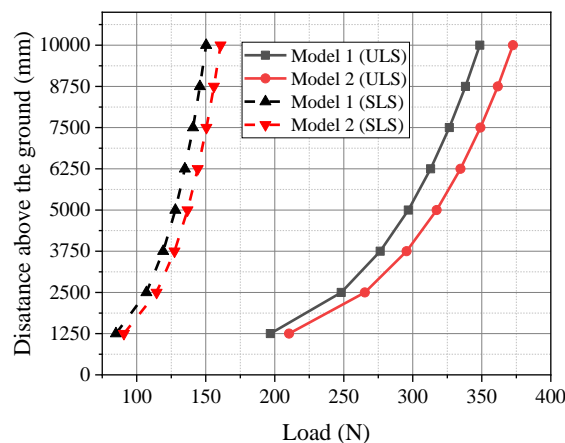


Fig. 4. ULS and SLS conditions load along the tower.

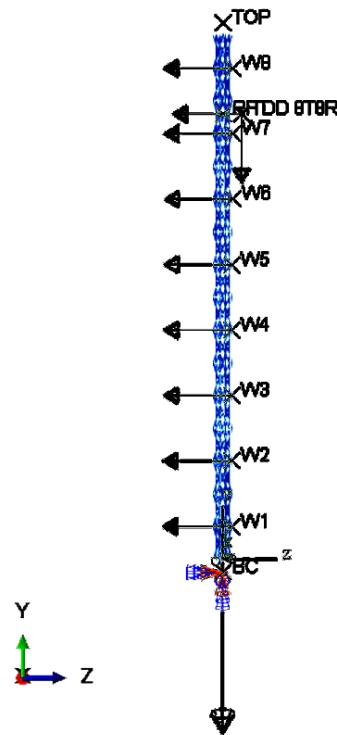


Fig. 5. Load pattern in ABAQUS.

4. Tower analysis and discussion

4.2. Strength verification

To ensure the tower's strength, it is important to evaluate the maximum stress it can withstand under different conditions. In the analysis, the ultimate limit state condition was considered, which assesses the tower's ability to withstand extreme loads and stresses.

The evaluation revealed that the highest stress values were mostly concentrated at the longitudinal members of the tower, specifically near the junctions where the longitudinal members meet the helical members and at the base of the tower. In Model 1 and Model 2, the maximum stress values were 135.6 MPa and 198.9 MPa, respectively, as shown in Fig. 6. These stress values represent the maximum stress the tower experienced under extreme loading conditions.

The concentration of stress in the longitudinal members can be attributed to the structural role these members play. Longitudinal members primarily carry axial loads, which are significantly influenced by bending moments and shear forces induced by wind loads. Due to their orientation and function, they experience higher stresses compared to other members. Additionally, the intersections of longitudinal and helical members create points of stress concentration, further amplifying the stress levels in the longitudinal members.

To determine whether the tower's strength met the necessary requirements, these stress values were compared to the design value of the carbon/epoxy material used in the tower's construction. This material's design value is 306 MPa, indicating that it can withstand stresses of up to 306 MPa without failing. The analysis showed that both Model 1 and Model 2 were well below this value, indicating that the tower's strength meets the necessary requirements for the ultimate limit state condition. This means that the tower can withstand extreme loads and stress without experiencing significant deformation or failure.

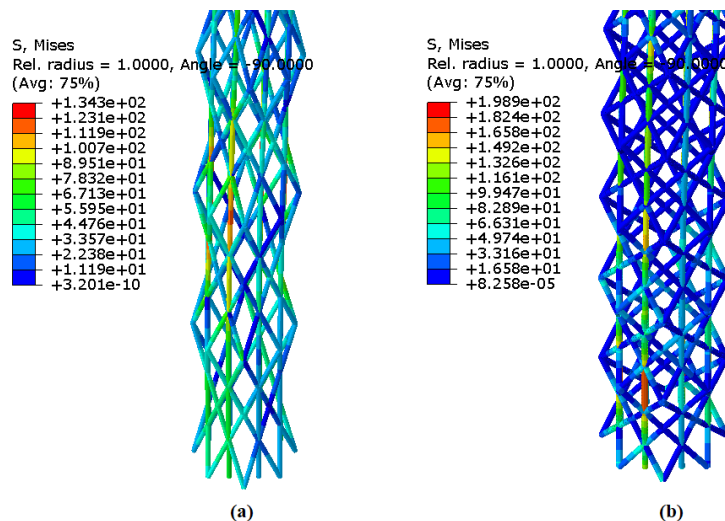


Fig. 6. Mises stress: (a) Model 1, (b) Model 2.

4.2. Stiffness verification

When constructing a tower, it is essential to ensure that it is stiff enough to withstand wind loads and other environmental factors. To verify the stiffness of the tower, engineers typically refer to industry standards like the TIA-222-G, which provide guidelines on maximum allowable displacement/height ratios for structures under various conditions. According to the TIA-222-G standard, the maximum displacement value for a tower's top under working wind speeds (serviceability limit state condition) should be less than 5%. This specification ensures that the tower can withstand normal wind loads without causing excessive deflection or deformation.

To determine whether the tower meets the TIA-222-G standard's requirements, an ABAQUS analysis was performed on two different models. The first model (Model 1) exhibited a displacement value of 0.045 m at a height of 10 meters, while the second model (Model 2) exhibited a displacement value of 0.047 m at the same height. The displacement ratio was calculated by dividing the displacement value of each model by the height of the tower ($0.045/10 = 4.5\%$ and $0.047/10 = 4.7\%$). Both models showed displacement ratios below the TIA-222-G standard's maximum limit of 5%, indicating that the stiffness of the tower is adequate for normal wind loads.

In Fig. 7 and Fig. 8, the displacement of the two models is graphically presented. These figures illustrate the deformation of the tower along its height. Both towers displayed identical displacements up to a height of approximately 6 m. Beyond this point, slight differences in deformation were observed, likely due to variations in the isotruss configuration and wind load distribution.

The displacement ratios of 4.5% (Model 1) and 4.7% (Model 2) are relatively sensitive to changes in wind speed and tower geometry. An increase in wind speed would result in higher wind pressures and consequently greater displacements, potentially exceeding the allowable limits. Similarly, changes in tower geometry, such as variations in the cross-sectional area or the length of the members, would alter the stiffness and deflection characteristics of the structure. Additionally, FRP materials exhibit elastic behavior until failure, which can result in sudden and catastrophic failure under high wind loads. To mitigate this risk, the design process should incorporate safety factors and robust design practices to ensure the structure remains within safe operational limits.

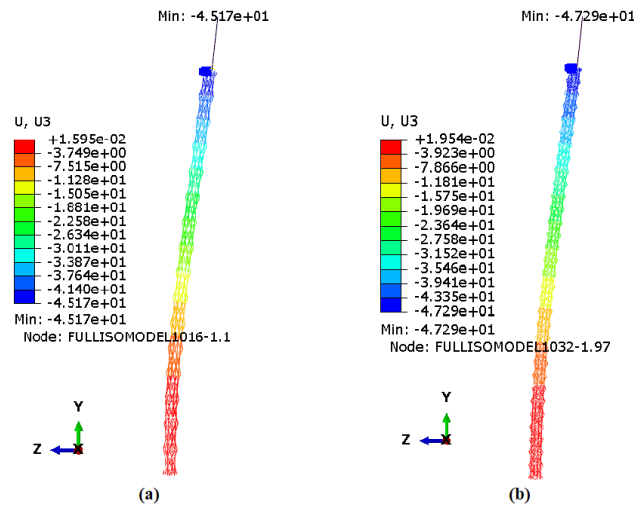


Fig. 7. Deflected shape under service load: (a) Model 1; (b) Model 2.

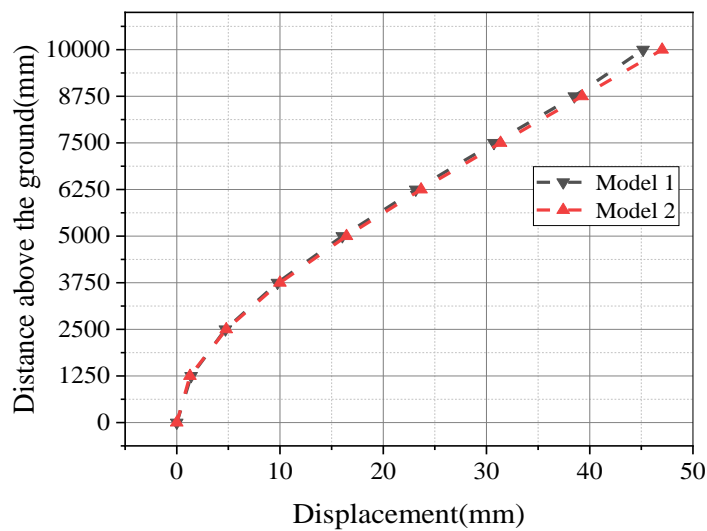


Fig. 8. Horizontal displacement of the tower versus height under wind load conditions.

4.3. Stability verification

To assess the stability of the structure, a buckling eigenvalue analysis was conducted using the Lanczos method. This involved calculating the first three modes of the structure and determining the corresponding buckling eigenvalues, which provide information on the structure's tendency to buckle or deform under loading conditions.

In Model 1, the buckling eigenvalues for the first three modes were 5.260, -5.303, and 5.379, respectively. In Model 2, the values were 8.420, -8.486, and 8.548. The analysis revealed that the primary mode of instability was local buckling in the longitudinal members, as illustrated in Fig. 9. Despite this instability, the analysis showed that the structure's stability met the necessary requirements for the given loading conditions, indicating that it can withstand the expected loads without experiencing significant deformation or failure.

The local buckling in the longitudinal members is attributed to their slenderness ratio, making them prone to buckling under axial loads. This finding is critical for refining and optimizing the design to ensure that the structure remains stable and safe under different loading conditions. Potential mitigation strategies to address this issue include increasing the cross-sectional area of the

longitudinal members, reducing their effective length by adding intermediate supports, decreasing the bay length, or using materials with a higher modulus of elasticity. These strategies can improve the buckling resistance and overall stability of the structure. decreasing the bay length or using materials with a higher modulus of elasticity. These strategies can improve the buckling resistance and overall stability of the structure.

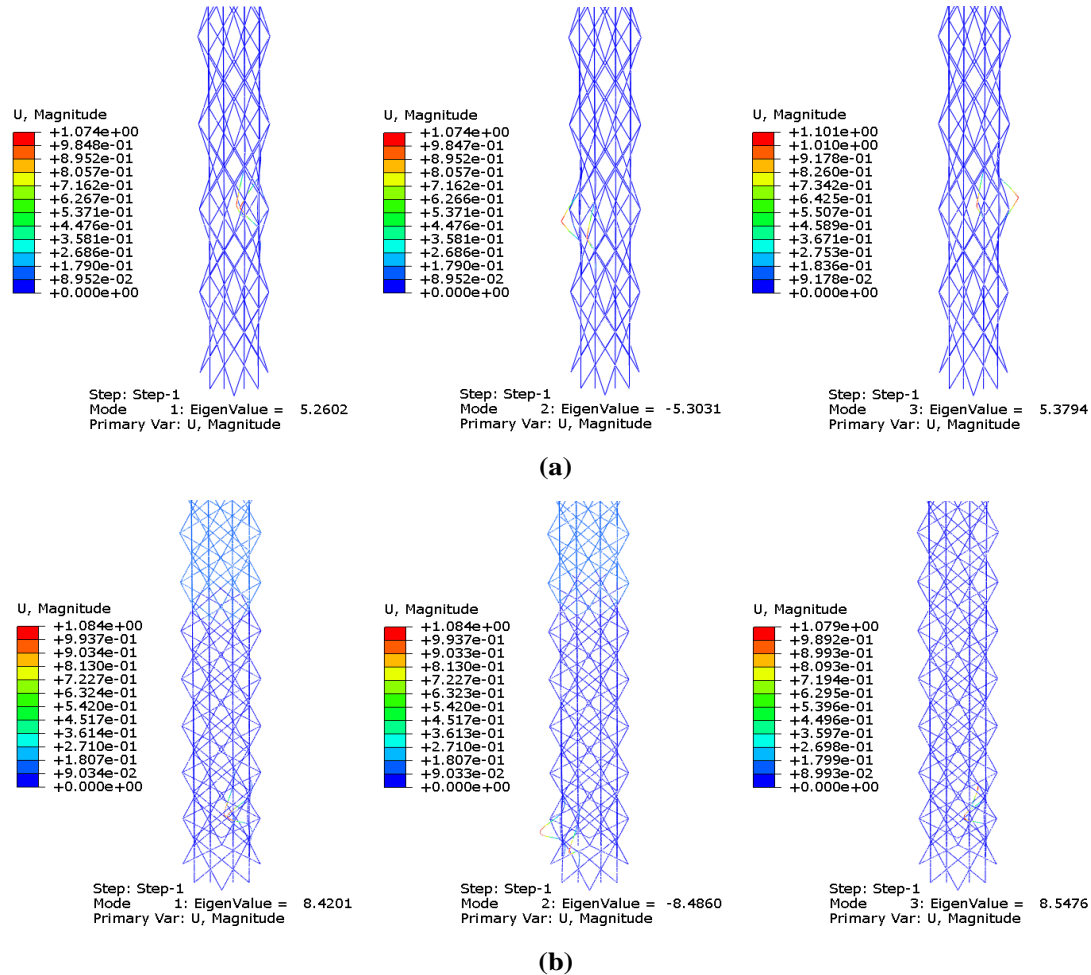


Fig. 9. Buckling analysis modes: (a) Model 1, (b) Model 2.

5. Conclusion

In summary, the investigation into self-supporting isotrussed telecommunication towers (SSITT) under wind loads, guided by the TIA-222-G standard, offers vital insights into their structural performance. Utilizing advanced composite materials and ABAQUS finite element software, the models demonstrated compliance with industry standards across various parameters. The stiffness verification confirmed the towers' capacity to withstand normal wind loads, with displacement ratios comfortably below the 5% limit specified by TIA-222-G. Concurrently, the ultimate limit state strength analysis showcased robustness as stress values in both models remained well within the safe limits of the material used.

While local buckling in the longitudinal member emerged as the primary instability mode, the stability analysis confirmed that the towers could endure expected loads without significant deformation or failure. The graphical representation of tower deformation illustrates the displacement behavior under wind loads, supporting the analysis outcomes. This visual

representation, combined with the stress and buckling analysis, provides a comprehensive understanding of the tower's performance.

In conclusion, the study underscores the resilience of SSITTs constructed with advanced composite materials, specifically carbon/epoxy, offering a stable and durable solution for telecommunication applications. Compliance with industry standards and identified areas for refinement, particularly reinforcing the longitudinal member, positions SSITTs for optimal performance, ensuring stability, and safety under diverse loading conditions.

6. Limitations and future research directions

To broaden the impact of this work, future research should consider modifying tower designs for different wind load scenarios, such as varying terrain or extreme weather events, to ensure structural stability. Additionally, the choice of material significantly influences stability and performance, with different outcomes expected from using other FRP materials like glass/epoxy. Scaling to taller structures would require consideration of additional factors like increased wind loads and dynamic effects. Furthermore, addressing other factors that affect the integrity of SSITT, such as soil durability, environmental conditions, material degradation, and accidental impacts, will provide a more holistic understanding of the tower's performance and longevity. Finally, a detailed economic analysis, including life-cycle cost assessment and sustainability considerations, should be conducted to determine the feasibility of using SSITT in practical applications.

Funding

This research did not receive any specific grant from funding agencies in the public, commercial, or not-for-profit sectors.

Conflict of interest

The authors declare no known competing financial interests or personal relationships that could have influenced the work reported in this paper.

References

- [1] Qureshi J. Fibre-Reinforced Polymer (FRP) in Civil Engineering. *Next Gener Fiber-Reinforced Compos - New Insights* 2023. <https://doi.org/10.5772/intechopen.107926>.
- [2] Correia JR, Bai Y, Keller T. A review of the fire behaviour of pultruded GFRP structural profiles for civil engineering applications. *Compos Struct* 2015;127:267–87. <https://doi.org/10.1016/j.compstruct.2015.03.006>.
- [3] Zaman A, Gutub SA, Wafa MA. A review on FRP composites applications and durability concerns in the construction sector. *J Reinf Plast Compos* 2013;32:1966–88. <https://doi.org/10.1177/0731684413492868>.
- [4] Hastak M, Mirmiran A, Richard D. A framework for life-cycle cost assessment of composites in construction. *J Reinf Plast Compos* 2003;22:1409–29. <https://doi.org/10.1177/073168403035586>.
- [5] Hu W, Li Y, Yuan H. Review of Experimental Studies on Application of FRP for Strengthening of Bridge Structures. *Adv Mater Sci Eng* 2020;2020. <https://doi.org/10.1155/2020/8682163>.

- [6] Polyzois DJ, Raftoyiannis IG, Ochonski A. Experimental and analytical study of latticed structures made from FRP composite materials. *Compos Struct* 2013;97:165–75. <https://doi.org/10.1016/j.compstruct.2012.10.032>.
- [7] Harle SM. Durability and long-term performance of fiber reinforced polymer (FRP) composites: A review. *Structures* 2024;60. <https://doi.org/10.1016/j.istruc.2024.105881>.
- [8] Lee LS, Jain R. The role of FRP composites in a sustainable world. *Clean Technol Environ Policy* 2009;11:247–9. <https://doi.org/10.1007/s10098-009-0253-0>.
- [9] Abbood IS, Odaa SA, Hasan KF, Jasim MA. Properties evaluation of fiber reinforced polymers and their constituent materials used in structures - A review. *Mater Today Proc* 2021;43:1003–8. <https://doi.org/10.1016/j.matpr.2020.07.636>.
- [10] Maiti S, Islam MR, Uddin MA, Afroj S, Eichhorn SJ, Karim N. Sustainable Fiber-Reinforced Composites: A Review. *Adv Sustain Syst* 2022;6. <https://doi.org/10.1002/adsu.202200258>.
- [11] Waghmare S, Shelare S, Aglawe K, Khope P. A mini review on fibre reinforced polymer composites. *Mater Today Proc* 2022;54:682–9. <https://doi.org/10.1016/j.matpr.2021.10.379>.
- [12] Sharma S, Sudhakara P, Nijjar S, Saini S, Singh G. Recent Progress of Composite Materials in various Novel Engineering Applications. *Mater Today Proc* 2018;5:28195–202. <https://doi.org/10.1016/j.matpr.2018.10.063>.
- [13] mahboubizadeh S, Sadeq A, Arzaqi Z, Ashkani O, Samadoghli M. Advancements in fiber-reinforced polymer (FRP) composites: an extensive review. *Discov Mater* 2024;4. <https://doi.org/10.1007/s43939-024-00091-9>.
- [14] Alshurafa S, Polyzois D. Design recommendations and comparative study of FRP and steel guyed towers. *Eng Sci Technol an Int J* 2018;21:807–14. <https://doi.org/10.1016/j.jestch.2018.06.014>.
- [15] Alshurafa SA, Polyzois D. An experimental and numerical study into the development of FRP guyed towers. *Compos Struct* 2018;201:779–90. <https://doi.org/10.1016/j.compstruct.2018.06.056>.
- [16] TIA Standard. ANSI-TIA-222-G-2005: Structural standard for antenna supporting structures and antennas. Washington DC, USA: Telecommunications Industry Association; 2006.
- [17] CEN. Eurocode 3: Design of steel structures : Towers, masts and chimneys - Towers and masts, 2006.
- [18] GB50135. GB 50135-2006: Code for design of high-rising structures, 2006.
- [19] CSA. CSA S37-18: Antennas, towers, and antenna-supporting structures., 2018.
- [20] IsoTruss. IsoTruss, Inc – A structural revolution 2023.
- [21] Jensen, David W, Larry R. Francom. Iso-Truss Structure. EP 1 358 392 B1, 2012.
- [22] Opdahl HB, Jensen DW. Dimensional analysis and optimization of isotruss structures with outer longitudinal members in uniaxial compression. *Materials (Basel)* 2021;14. <https://doi.org/10.3390/ma14082079>.
- [23] Fan HL, Meng FH, Yang W. Mechanical behaviors and bending effects of carbon fiber reinforced lattice materials. *Arch Appl Mech* 2006;75:635–47. <https://doi.org/10.1007/s00419-006-0032-x>.
- [24] Gaikwad AA, Kenjale AC, Bhosale AB, Dumbre T V, Arakerimath RR, Roy S. Design Analysis & Manufacturing Of Carbon Composite Isotruss For Bending Analysis. *Int Conf Recent Adv Mech Eng* 2015:133–6.
- [25] Sui Q, Fan H, Lai C. Failure analysis of 1D lattice truss composite structure in uniaxial compression. *Compos Sci Technol* 2015;118:207–16. <https://doi.org/10.1016/j.compscitech.2015.09.003>.
- [26] M G, S R. Buckling Characteristics Study of Isotruss Structure with Different Positions of Longitudinal Members. *Int J Cybern Informatics* 2016;5:217–25. <https://doi.org/10.5121/ijci.2016.5121>.
- [27] Richardson S. In-Situ Testing of a Carbon/Epoxy IsoTruss Reinforced Concrete Foundation Pile. Brigham Young University, 2006.
- [28] Rackliffe ME, Jensen DW, Lucas WK. Local and global buckling of ultra-lightweight IsoTruss® structures. *Compos Sci Technol* 2006;66:283–8. <https://doi.org/10.1016/j.compscitech.2005.04.038>.

- [29] Sui Q, Fan H, Manufacturing I. Vibration Behaviors of the IsoTruss ® Composite Structure. 21st Int. Conf. Compos. Mater., 2017, p. 1–4.
- [30] Jensen DW, Hinds KB. Shear-dominated bending behavior of carbon/epoxy composite lattice isobeam structures. ICCM Int Conf Compos Mater 2015;2015-July:19–24.
- [31] Asay BA. Bending Behavior of Carbon / Epoxy Composite IsoBeam Structures. Brigham Young University, 2015.
- [32] Hinds KB. Shear-dominated bending behavior of carbon/epoxy composite lattice isobeam structures. vol. 2015-July. Provo, Utah: 2015.
- [33] Ferrell MJ. Flexural Behavior of Carbon/Epoxy IsoTruss Reinforced-Concrete Beam-Columns. Brigham Young University, 2005.
- [34] Gaufin T. Design of a Composite Bridge for Aspen Grove. Brigham Young University, 1999.
- [35] Delta7 Bikes n.d.
- [36] Lai C. Mechanical properties and fabrication of composite grid structures. Northwestern Polytechnical University, 2015.
- [37] Opdahl Hanna Belle. Investigation of IsoTruss ® Structures in Compression Using Numerical , Dimensional , and Optimization Methods. Brigham Young University, 2020.
- [38] Ayers JT. Hydrodynamic Drag and Flow Visualization of IsoTruss Lattice Structures. Brigham Young University, 2005.
- [39] Hansen SM, Jensen DW. Influence of consolidation and interweaving on compression behavior of IsoTrussTM structures. Inst Phys Conf Ser 2003;180:83–92.
- [40] Lai C, Sui Q, Fan H. Designing Hierarchical IsoTruss Column Based on Controlling Multi-Buckling Behaviors. Int J Struct Stab Dyn 2022;22:1–19. <https://doi.org/10.1142/S0219455422500304>.
- [41] Rackliffe ME. Development of Ultra-lightweight IsoTrussTM Grid Structures. Brigham Young University, 2002.
- [42] IsoTruss. Sustainability: Eco-friendly – IsoTruss, Inc 2023.
- [43] Rasool AM, Qureshi MU, Ahmad M. A Comparative Study on the Calculation of Wind Load and Analysis of Communication Tower as per TIA-222-G and TIA-222-H Standards. KSCE J Civ Eng 2021;25:646–53. <https://doi.org/10.1007/s12205-020-0662-5>.
- [44] Smith M. ABAQUS/Standard User’s Manual, Version 6.9 2009.